Supplemental Materials

Molecular Biology of the Cell

Trexler et al.

SI Figure 1

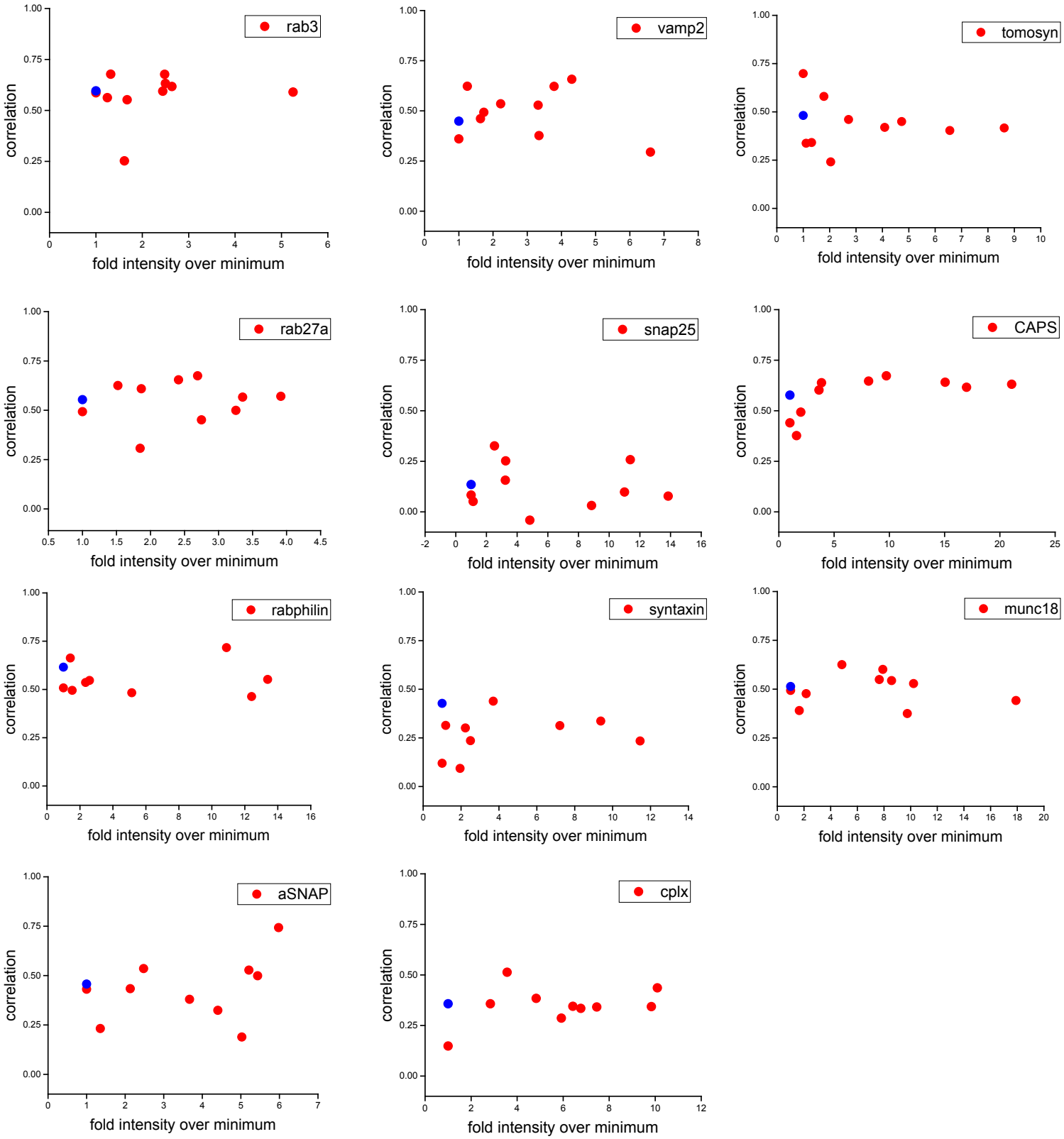

SI Figure 1: Protein overexpression level does not affect correlation values. Cells expressing the indicated constructs were imaged on one coverslip under carefully controlled conditions with the same illumination intensity and TIRF illumination profile. Under this setup, we use average pixel fluorescence intensity from cells (background subtracted from an adjacent region in the field of view) as a proxy for expression level. We normalized intensity to the minimum intensity from the dataset (set to 1) and plotted this against the mean correlation value obtained from that cell according to the correlation analysis described in the text. The blue datapoint is the average correlation value from the entire dataset for that construct (given in Figure 2) for comparison plotted at x=1.

SI Figure 2

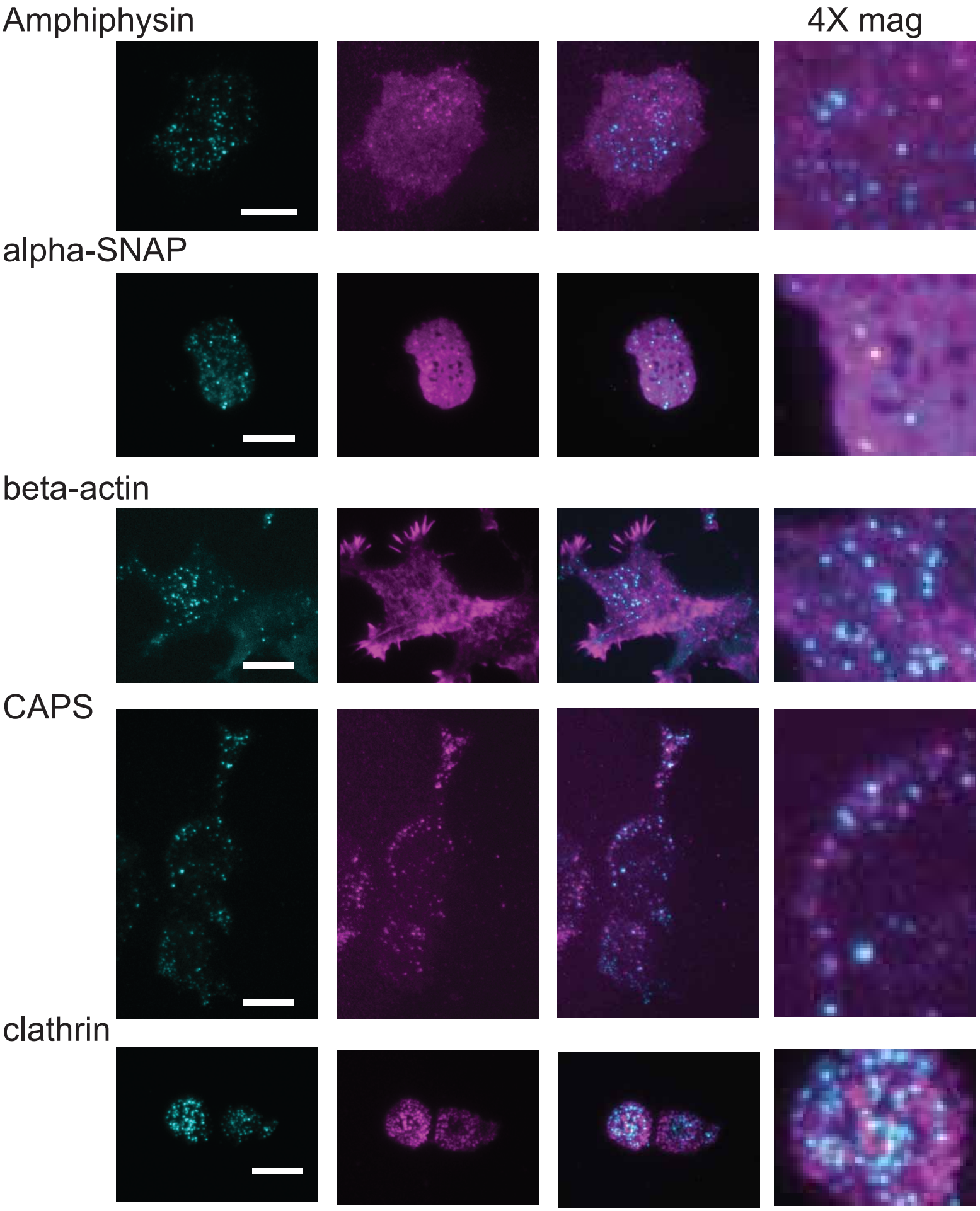

SI Figure 2

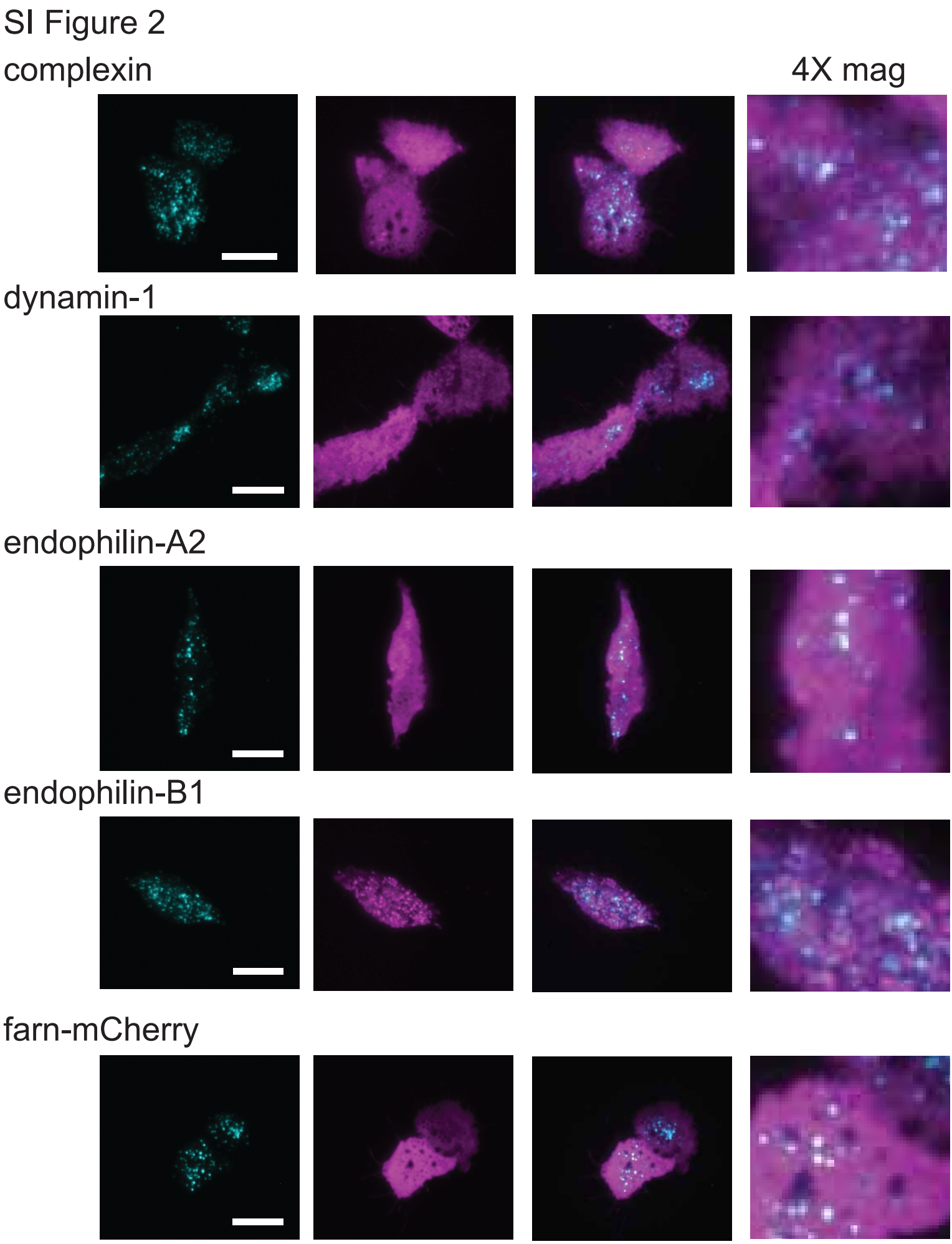
complexin
4X mag
dynamin-1
endophilin-A2
endophilin-B1
farn-mCherry

SI Figure 2

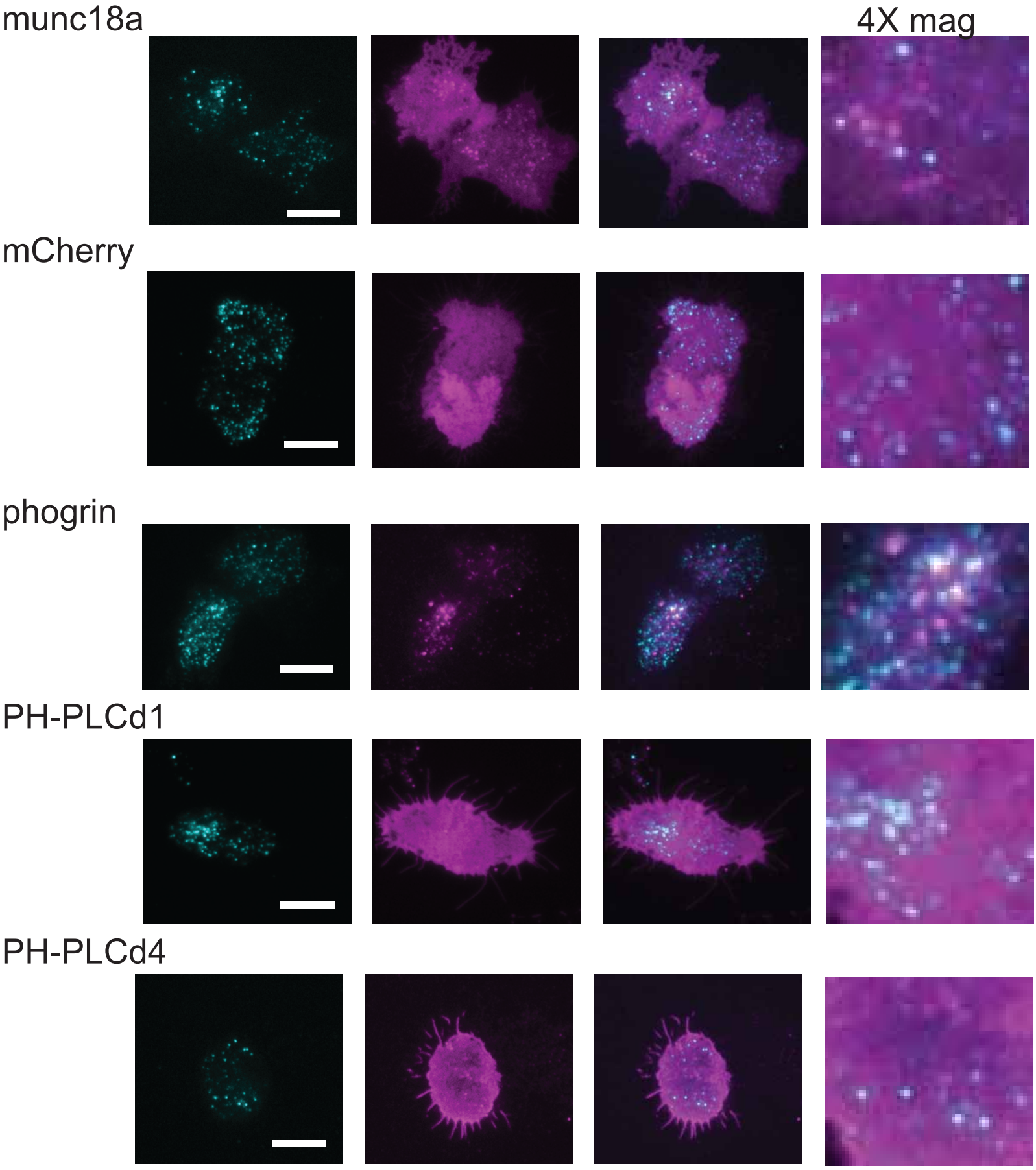

SI Figure 2

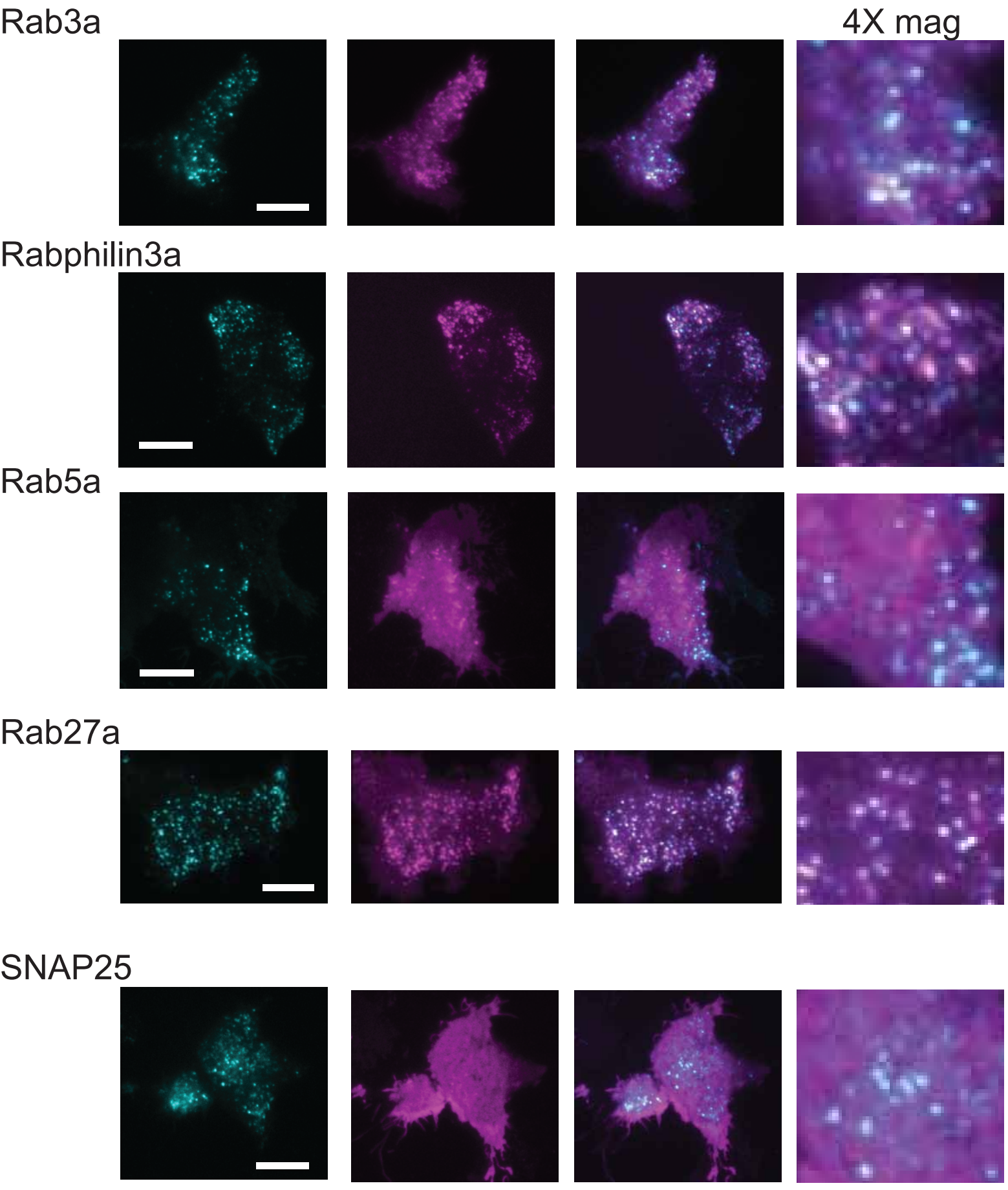

SI Figure 2

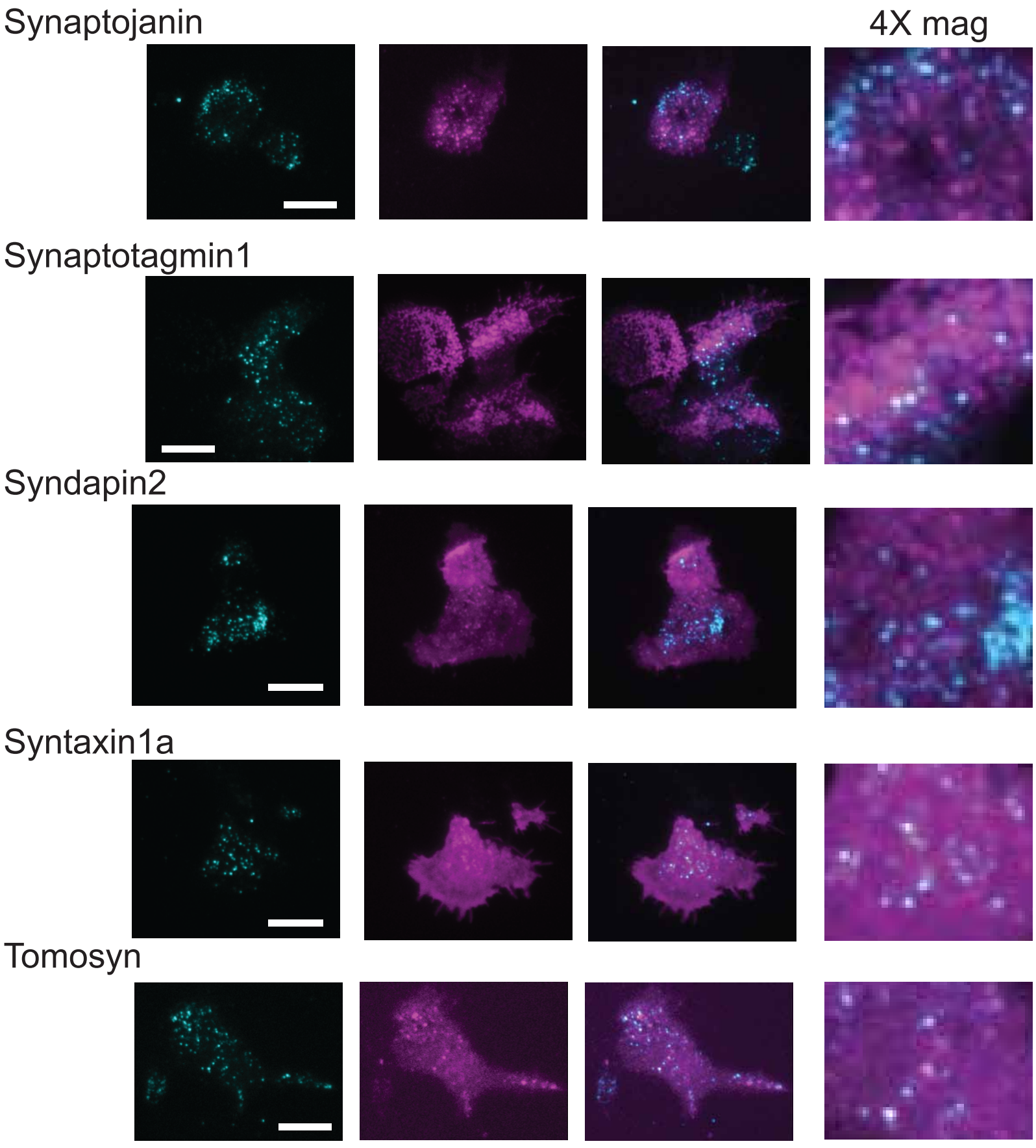
Synaptojanin
4X mag
Synaptotagmin1
Syndapin2
Syntaxin1a
Tomosyn

SI Figure 2

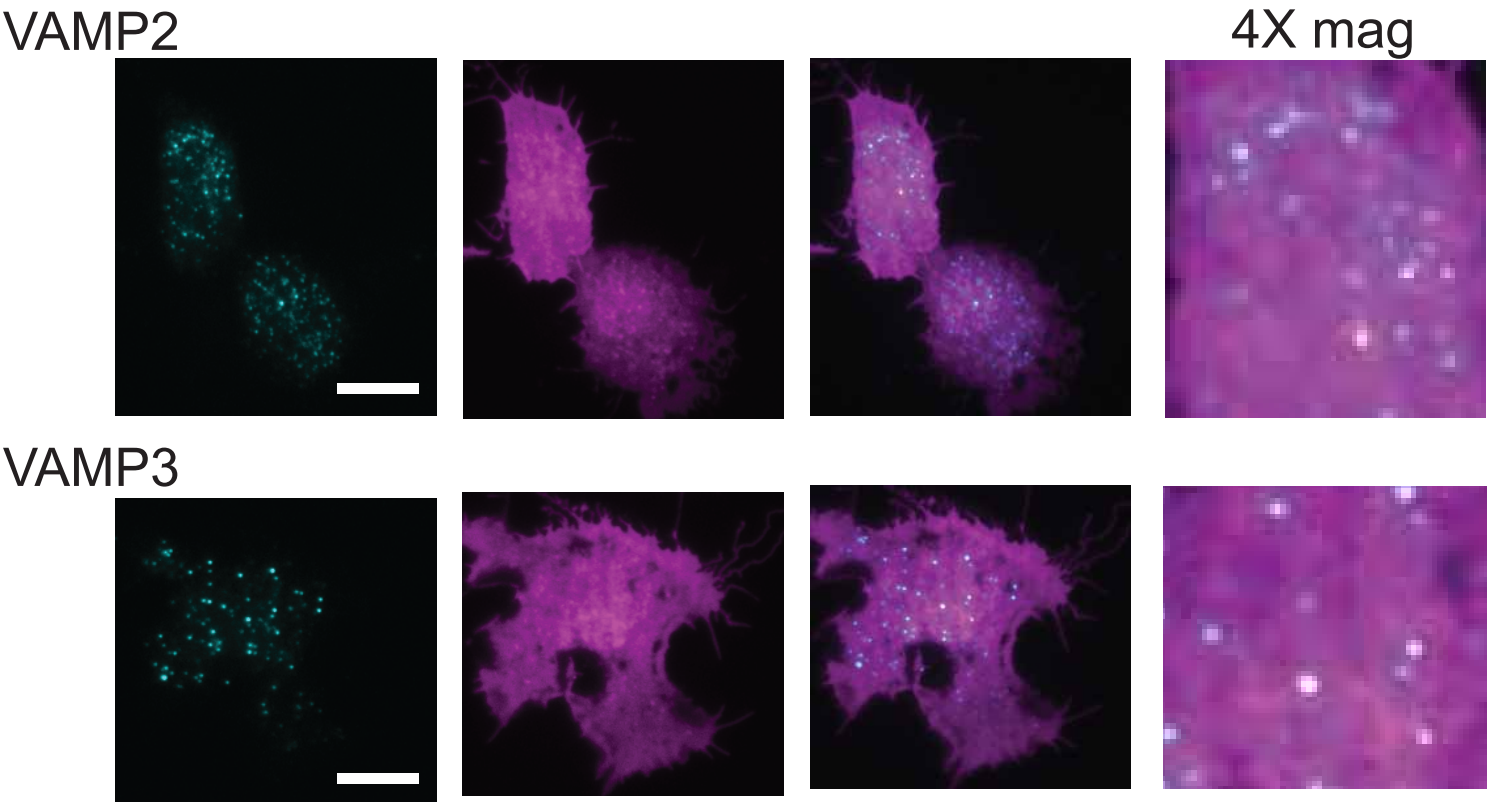

SI Figure 2: Gallery of representative TIRF images from all cells imaged. From left to right in each row: cyan image of NPY-GFP, magenta image of the red-labeled test protein, merge of both channels, and a 4X magnification of the merged image to better show colocalization patterns. Scale bars are 10 μm.

SI Figure 3

A

	rabphilin3a	rab3	CAPS	rab27a	munc18	tomosyn	alphaSNAP	VAMP2	syntaxin1a	rab5a	complexin	endophilinB1	VAMP3	phogrin	OCRL	synaptotagmin	endophilinA2	syndapin	clathrin	SNAP25	synaptojanin	dynamin-1	fcho2	Ph-PLCd4	mCherry alone	amphiphysin	farn-mCherry	PH-PLC	dynamin-2	actin
rabphilin3a	1	0.019312	3.156E-05	5.746E-10	1.681E-28	2.25E-38	3.197E-40	3.166E-58	3.459E-52	6.76E-108	2.01E-115	8.125E-79	2.94E-121	1.75E-113	2.45E-141	6.56E-104	2.56E-143	3.27E-149	2.64E-145	2.43E-235	3.26E-130	1.17E-165	2.14E-159	1.06E-231	3.68E-201	2.31E-248	6.31E-148	1E-261	6E-212	0
rab3	0.019312	1	0.0234814	2.663E-06	2.775E-23	9.553E-36	3.983E-39	1.458E-56	1.539E-52	2.78E-114	5.63E-123	1.104E-82	3.2E-128	1.96E-121	1.42E-152	2.75E-112	2.79E-160	6.01E-170	2.15E-161	9.24E-266	7.68E-144	2.99E-188	4.54E-178	8.61E-264	1.25E-230	9.06E-284	1.19E-168	4E-299	6E-243	0
CAPS	3.156E-05	0.0234814	1	0.0117705	1.338E-13	2.684E-27	7.076E-31	3.35E-42	5.944E-42	6.846E-98	3.46E-105	3.485E-62	4.82E-99	1.851E-97	1.76E-122	6.042E-89	8.93E-145	9.95E-160	2.57E-131	1.56E-241	3.2E-111	1.5E-165	3.95E-144	7.83E-242	2.63E-215	6.18E-269	1.46E-146	2E-275	3E-212	0
rab27a	5.746E-10	2.663E-06	0.0117705	1	9.824E-06	1.532E-14	2.198E-18	7.175E-26	3.69E-27	1.068E-69	3.793E-76	4.592E-46	2.316E-74	2.293E-73	1.264E-94	1.953E-68	8.45E-114	7.08E-128	7.1E-106	4.76E-198	1.664E-90	4.07E-135	7.5E-118	1.18E-199	5.68E-177	1.88E-222	6.47E-120	6E-230	3E-177	0
munc18	1.681E-28	2.775E-23	1.338E-13	9.824E-06	1	0.0002857	4.906E-08	1.911E-12	2.096E-15	1.672E-50	1.595E-57	3.56E-38	5.859E-63	3.832E-62	4.768E-85	1.423E-61	1.04E-103	1.74E-120	1.68E-105	2.82E-195	1.845E-93	1.43E-135	2.02E-121	3.91E-200	5.73E-176	1.36E-220	5.86E-122	2E-235	4E-187	0
tomosyn	2.25E-38	9.553E-36	2.684E-27	1.532E-14	0.0002857	1	0.0154142	0.0005953	6.993E-07	1.164E-31	6.184E-37	2.808E-21	2.721E-36	3.155E-38	6.182E-54	1.074E-38	9.433E-82	4.75E-104	9.089E-73	6.1E-161	1.683E-61	3.2E-106	9.892E-85	6.73E-169	5.71E-153	1.11E-197	1.893E-94	1E-202	3E-149	0
alphaSNAP	3.197E-40	3.983E-39	7.076E-31	2.198E-18	4.906E-08	0.0154142	1	0.4456174	0.0194731	3.676E-15	1.157E-18	2.786E-12	4.851E-21	3.24E-22	3.308E-33	5.002E-24	9.347E-51	2.284E-66	2.596E-49	8.11E-108	4.495E-43	5.07E-72	5.457E-59	1.48E-114	1.25E-102	7.64E-133	8.594E-65	6E-140	2E-105	2E-246
VAMP2	3.166E-58	1.458E-56	3.35E-42	7.175E-26	1.911E-12	0.0005953	0.4456174	1	0.0662382	6.409E-15	4.287E-19	1.592E-14	3.475E-25	5.429E-26	1.201E-40	1.679E-29	1.353E-57	1.889E-74	1.133E-63	4.48E-128	3.45E-58	1.354E-88	9.186E-78	2.31E-136	8.78E-120	1.41E-152	7.204E-81	1E-167	2E-133	2E-275
syntaxin1a	3.459E-52	1.539E-52	5.944E-42	3.69E-27	2.096E-15	6.993E-07	0.0194731	0.0662382	1	8.314E-07	2.945E-09	1.48E-07	4.035E-13	5.596E-14	4.935E-23	7.07E-17	5.375E-36	3.387E-49	6.852E-40	1.842E-85	1.486E-36	2.162E-58	1.015E-49	1.273E-92	8.125E-82	1.13E-105	1.904E-53	4E-116	1.3E-90	1E-203
rab5a	6.76E-108	2.78E-114	6.846E-98	1.068E-69	1.672E-50	1.164E-31	3.676E-15	6.409E-15	8.314E-07	1	0.1949156	0.0179575	0.0001579	2.164E-05	1.93E-12	1.679E-09	3.444E-25	4.727E-41	1.957E-34	7.552E-78	3.753E-34	5.176E-55	2.978E-47	1.927E-89	6.156E-79	2.89E-102	4.1E-52	7E-119	8.8E-97	1E-219
complexin	2.01E-115	5.63E-123	3.46E-105	3.793E-76	1.595E-57	6.184E-37	1.157E-18	4.287E-19	2.945E-09	0.1949156	1	0.1352063	0.0072691	0.0014816	2.354E-09	2.654E-07	2.287E-20	5.999E-35	1.657E-30	6.9E-69	3.142E-31	2.081E-49	3.591E-43	1.756E-80	1.195E-70	1.806E-91	2.33E-47	6E-109	2E-90	2E-202
endophilinB1	8.125E-79	1.104E-82	3.485E-62	4.592E-46	3.56E-38	2.808E-21	2.786E-12	1.592E-14	1.48E-07	0.0179575	0.1352063	1	0.5227151	0.2984669	0.0011467	0.0042143	1.308E-07	1.15E-13	1.361E-16	6.645E-32	1.12E-19	1.263E-24	8.92E-26	1.306E-38	4.712E-32	8.038E-41	1.665E-24	1.5E-55	8.5E-52	2.7E-96
VAMP3	2.94E-121	3.2E-128	4.82E-99	2.316E-74	5.859E-63	2.721E-36	4.851E-21	3.475E-25	4.035E-13	0.0001579	0.0072691	0.5227151	1	0.5740826	0.000981	0.0032079	2.573E-09	3.216E-18	2.396E-22	8.845E-44	2.935E-27	3.338E-34	6.965E-36	9.131E-54	8.943E-45	6.193E-57	1.98E-34	6.1E-78	7.3E-74	1E-134
phogrin	1.75E-113	1.96E-121	1.851E-97	2.293E-73	3.832E-62	3.155E-38	3.24E-22	5.429E-26	5.596E-14	2.164E-05	0.0014816	0.2984669	0.5740826	1	0.0119147	0.0221808	1.608E-07	1.368E-15	1.21E-17	6.394E-37	3.49E-21	1.192E-28	1.64E-28	4.899E-46	7.098E-39	8.435E-50	6.728E-29	2.4E-67	3E-62	1E-122
OCRL	2.45E-141	1.42E-152	1.76E-122	1.264E-94	4.768E-85	6.182E-54	3.308E-33	1.201E-40	4.935E-23	1.93E-12	2.354E-09	0.0011467	0.000981	0.0119147	1	0.8131336	0.0018294	6.722E-10	1.003E-12	4.526E-27	9.283E-18	1.548E-22	6.759E-24	1.235E-36	1.438E-30	5.238E-39	6.091E-24	6.6E-58	7.5E-58	1E-108
synaptotagmin	6.56E-104	2.75E-112	6.042E-89	1.953E-68	1.423E-61	1.074E-38	5.002E-24	1.679E-29	7.07E-17	1.679E-09	2.654E-07	0.0042143	0.0032079	0.0221808	0.8131336	1	0.018549	9.919E-07	1.244E-08	3.826E-18	4.239E-12	2.902E-15	3.239E-16	8.729E-25	1.099E-20	2.304E-26	2.768E-16	1.1E-39	7.9E-40	4.1E-76
endophilinA2	2.56E-143	2.79E-160	8.93E-145	8.45E-114	1.04E-103	9.433E-82	9.347E-51	1.353E-57	5.375E-36	3.444E-25	2.287E-20	1.308E-07	2.573E-09	1.608E-07	0.0018294	0.018549	1	0.0010479	0.0002953	2.114E-11	6.59E-07	2.34E-10	8.432E-10	2.662E-18	4.47E-16	6.546E-21	6.945E-12	1.4E-32	2E-32	7.2E-78
syndapin	3.27E-149	6.01E-170	9.95E-160	7.08E-128	1.74E-120	4.75E-104	2.284E-66	1.889E-74	3.387E-49	4.727E-41	5.999E-35	1.15E-13	3.216E-18	1.368E-15	6.722E-10	9.919E-07	0.0010479	1	0.5238814	0.011554	0.0192962	0.0020554	0.0020278	2.608E-06	9.174E-06	2.217E-07	9.472E-05	1.2E-14	5E-17	7E-45
clathrin	2.64E-145	2.15E-161	2.57E-131	7.1E-106	1.68E-105	9.089E-73	2.596E-49	1.133E-63	6.852E-40	1.957E-34	1.657E-30	1.361E-16	2.396E-22	1.21E-17	1.003E-12	1.244E-08	0.0002953	0.5238814	1	0.1157392	0.0268532	0.0150851	0.0038117	0.0001822	0.0006586	8.823E-05	0.0006651	7.8E-12	2.1E-17	4.4E-32
SNAP25	2.43E-235	9.24E-266	1.56E-241	4.76E-198	2.82E-195	6.1E-161	8.11E-108	4.48E-128	1.842E-85	7.552E-78	6.9E-69	6.645E-32	8.845E-44	6.394E-37	4.526E-27	3.826E-18	2.114E-11	0.011554	0.1157392	1	0.2348234	0.1252468	0.0613255	0.0027951	0.0045273	0.0008283	0.0034449	4.4E-12	1.1E-18	1.3E-44
synaptojanin	3.26E-130	7.68E-144	3.2E-111	1.664E-90	1.845E-93	1.683E-61	4.495E-43	3.45E-58	1.486E-36	3.753E-34	3.142E-31	1.12E-19	2.935E-27	3.49E-21	9.283E-18	4.239E-12	6.59E-07	0.0192962	0.0268532	0.2348234	1	0.9412889	0.6813292	0.4190763	0.4314436	0.3426687	0.2518399	0.00054	1.8E-08	7.3E-14
dynamin-1	1.17E-165	2.99E-188	1.5E-165	4.07E-135	1.43E-135	3.2E-106	5.07E-72	1.354E-88	2.162E-58	5.176E-55	2.081E-49	1.263E-24	3.338E-34	1.192E-28	1.548E-22	2.902E-15	2.34E-10	0.0020554	0.0150851	0.1252468	0.9412889	1	0.7445335	0.389596	0.3815919	0.2814902	0.2208012	8.8E-05	5.1E-09	2.2E-20
fcho2	2.14E-159	4.54E-178	3.95E-144	7.5E-118	2.02E-121	9.892E-85	5.457E-59	9.186E-78	1.015E-49	2.978E-47	3.591E-43	8.92E-26	6.965E-36	1.64E-28	6.759E-24	3.239E-16	8.432E-10	0.0020278	0.0038117	0.0613255	0.6813292	0.7445335	1	0.6602609	0.6300492	0.5360994	0.3536626	0.0006	6.4E-09	4.6E-16
Ph-PLCd4	1.06E-231	8.61E-264	7.83E-242	1.18E-199	3.91E-200	6.73E-169	1.48E-114	2.31E-136	1.273E-92	1.927E-89	1.756E-80	1.306E-38	9.131E-54	4.899E-46	1.235E-36	8.729E-25	2.662E-18	2.608E-06	0.0001822	0.0027951	0.4190763	0.389596	0.6602609	1	0.8983522	0.8035112	0.4717706	0.00021	8.3E-10	8.8E-25
mCherry alone	3.68E-201	1.25E-230	2.63E-215	5.68E-177	5.73E-176	5.71E-153	1.25E-102	8.78E-120	8.125E-82	6.156E-79	1.195E-70	4.712E-32	8.943E-45	7.098E-39	1.438E-30	1.099E-20	4.47E-16	9.174E-06	0.0006586	0.0045273	0.4314436	0.3815919	0.6300492	0.8983522	1	0.9248589	0.5814943	0.00137	1E-07	1.3E-20
amphiphysin	2.31E-248	9.06E-284	6.18E-269	1.88E-222	1.36E-220	1.11E-197	7.64E-133	1.41E-152	1.13E-105	2.89E-102	1.806E-91	8.038E-41	6.193E-57	8.435E-50	5.238E-39	2.304E-26	6.546E-21	2.217E-07	8.823E-05	0.0008283	0.3426687	0.2814902	0.5360994	0.8035112	0.9248589	1	0.5815383	0.00041	3.2E-09	6.9E-26
farn-mCherry	6.31E-148	1.19E-168	1.46E-146	6.47E-120	5.86E-122	1.893E-94	8.594E-65	7.204E-81	1.904E-53	4.1E-52	2.33E-47	1.665E-24	1.98E-34	6.728E-29	6.091E-24	2.768E-16	6.945E-12	9.472E-05	0.0006651	0.0034449	0.2518399	0.2208012	0.3536626	0.4717706	0.5814943	0.5815383	1	0.04849	5.5E-05	3.8E-11
PH-PLC	1.11E-261	3.61E-299	2.02E-275	5.65E-230	2.23E-235	1.43E-202	6.49E-140	1.17E-167	4E-116	7.44E-119	6.49E-109	1.469E-55	6.107E-78	2.37E-67	6.648E-58	1.068E-39	1.398E-32	1.203E-14	7.78E-12	4.393E-12	0.0005411	8.801E-05	0.0005999	0.0002119	0.0013697	0.0004125	0.0484907	1	0.00082	1.1E-10
dynamin-2	6.02E-212	6.4E-243	3.43E-212	3.33E-177	4.5E-187	2.74E-149	2.43E-105	1.94E-133	1.267E-90	8.762E-97	2.012E-90	8.464E-52	7.279E-74	2.961E-62	7.508E-58	7.864E-40	2.024E-32	5.012E-17	2.126E-17	1.102E-18	1.828E-08	5.051E-09	6.357E-09	8.337E-10	1.01E-07	3.213E-09	5.541E-05	0.00082	1	0.1102
actin	0	0	0	0	0	0	1.7E-246	1.99E-275	1.04E-203	1.22E-219	2.38E-202	2.747E-96	1.07E-134	9.9E-123	1.05E-108	4.079E-76	7.21E-78	6.976E-45	4.437E-32	1.335E-44	7.254E-14	2.187E-20	4.554E-16	8.809E-25	1.316E-20	6.945E-26	3.798E-11	1.1E-10	0.1102	1

B

Exocytic Constructs	Cells	Events
actin	4	24
amphiphysin	6	34
CAPS	4	49
clathrin light chain	8	45
complexin	3	21
dynamin1	4	50
dynamin1-K44A	4	29
dynamin1-K535A	10	39
dynamin1-S774E-S778E	4	43
dynamin1-833-838A	4	46
dynamin2	9	38
dynamin2-K535A	3	33
dynamin2-dPRD	7	18
endophilin A1	3	12
endophilin A2	4	45
endophilin B1	1	4
farnesylated-mCherry	4	26
mCherry	9	51
munc18a	5	31
NPY alone	4	19
phogrin	3	23
PH-PLCd1	3	15
PH-PLCd4	5	30
rab3a	3	37
rab5a	5	28
rab27a	5	50
rabphilin3a	3	31
SNAP25	3	33
synaptotagmin-1	4	26
syndapin2	5	41
syntaxin1a	7	28
tomosyn	5	38
VAMP3	5	40
alphaSNAP		
VAMP2		
OCRL		
FCHO2		
Avg	**4.73**	**32.64**

Plasmid	Source
mCherry-betaActin	C. Waterman (NHLBI, NIH)
Amph1-pmCherry-N1	C. Merrifield (addgene 27692)
CAPS-mKate2	T. Martin (UW-Madison)
mCherry-CLC-C1	W. Almers (OHSU)
Complexin2-mCherry-N1	biobasic synthesis
Dynamin1-mCherry-N1	C. Merrifield (addgene 27697)
Dynamin1-mCherry-N1	J. Taraska (NHLBI, NIH)
Dynamin1-mCherry-N1	J. Taraska (NHLBI, NIH)
Dynamin1-mCherry-N1	J. Taraska (NHLBI, NIH)
Dynamin1-mCherry-N1	J. Taraska (NHLBI, NIH)
Dynamin2-mCherry-N1	C. Merrifield (addgene 27689)
Dynamin2-mCherry-N2	J. Taraska (NHLBI, NIH)
Dynamin2-mCherry-N3	J. Taraska (NHLBI, NIH)
Endophilin A1-mCherry-N1	DNASU HsCD00000899
Endophilin A2-mCherry-N1	DNASU HsCD00005501
Endophilin B1-mCherry-N1	DNASU HsCD00042012
Farnesyl-5-mCherry	J. Taraska (NHLBI, NIH)
mCherry-N1	Clontech
mCherry-munc18-C1	Biobasic synthesis
NPY-EGFP-N1	W. Almers (OHSU)
Phogrin-mRFP	J. Taraska (NHLBI, NIH)
RFP-C1-PLCdelta-PH	B. Hille (UW)
PLCdelta4-mKate2	T. Martin (UW-Madison)
mRFP-Rab3a	M. Fukuda (Tohoku U.)
mCherry-Rab5a-C1	C. Merrifield (addgene 27679)
mCherry-Rab27a-C1	W. Westbroek (NIH, GFP-Rab27a)
mCherry-Raphillin3A-C1	I. Macara (VUMC, original vector GFP-Raphillin3A)
mCherry-SNAP25-C1	J. Taraska (NHLBI, NIH)
mCherry-synaptotagmin1	J. Taraska (NHLBI, NIH)
Syndapin2-mCherry-C1	C. Merrifield (addgene 27681)
Syntaxin1A-mCherry-N1	W. Almers (OHSU)
mCherry-Tomosyn-C1	Biobasic synthesis
VAMP3-mCherry-N1	M. Coppolinno (University of Guelph, EGFP-SNAP23)
alphaSNAP-mCherry-N1	P. Hanson (WUSL, original vector alphaSNAP-PET28a)
VAMP2-mCherry-N1	R. Scheller (Stanford, original vector VAMP2)
mCherry-ORCL1-C1	C. Merrifield (addgene 27675)
FCHo2-mCherry-C1	C. Merrifield (addgene 27686)

SI Figure 3: P-value table and protein/experiment data. (A) Pairwise calculation of P-values for every protein correlation dataset. The NPY-GFP correlation values of each protein (shown in Figure 2D) is compared to the correlation value dataset of every other protein using an unpaired two-tailed Student's T-Test. Blue indicates the P-value is below 0.001. On average the correlation value datasets n= 363 values from 8.2 cells and multiple independent experiments. (B) All proteins and plasmids used in this study. Sources of plasmids are indicated at right. For exocytic constructs, number of events and cells refers to the number of exocytic events analyzed to produce intensity trajectories and how many cells were used.

SI Figure 4

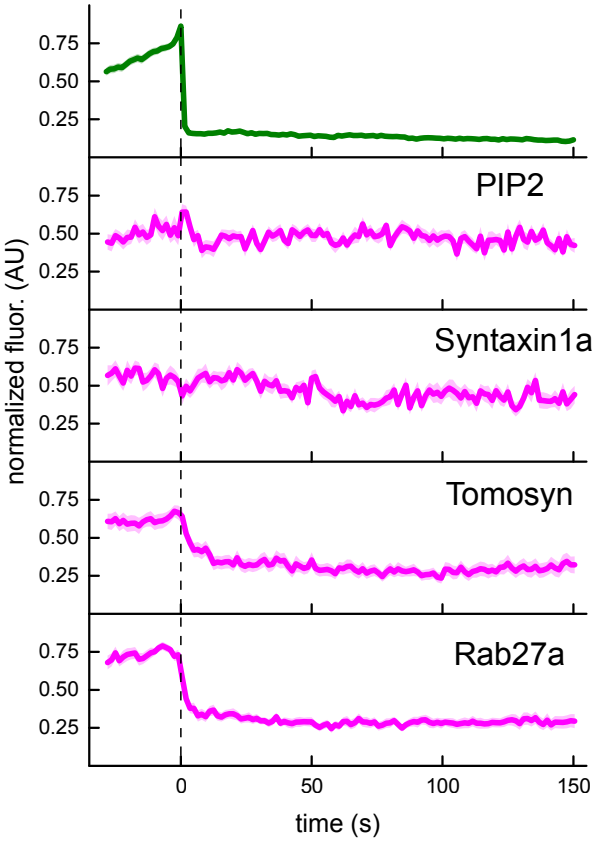

SI Figure 4: High potassium stimulation of exocytosis in INS-1 cells gives similar intensity trajectories as ionomycin stimulation. Cells were perfused as described for other stimulation experiments but with stimulation buffer instead of ionomycin. Background subtracted and normalized fluorescence intensity traces are shown for each protein indicated. The mean fluorescence intensity is shown as a dark line and the standard error of the dataset is shown in transparency behind the data. At top the average NPY-GFP signal for all events in this figure is shown as a relative standard of time (N=96). The dotted line marks time=0 for ease of trajectory comparison. The behaviors of each protein shown here are qualitatively very similar to the behaviors induced with ionomycin-stimulated exocytosis. PIP2 is transiently recruited near the time of membrane fusion. Rab27a and tomosyn are both stably present at the DCV before fusion and decay rapidly after exocytosis. Syntaxin1a appears to change very little upon exocytosis.

SI Figure 5

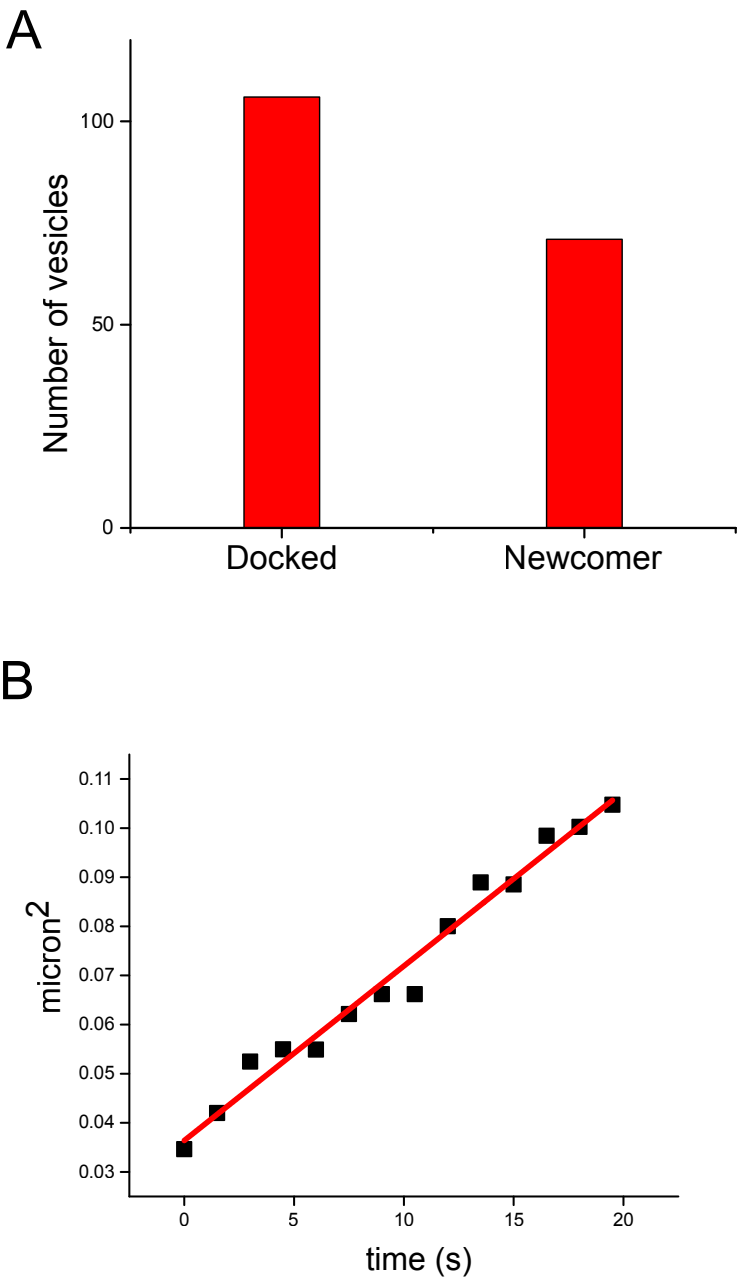

SI Figure 5: A majority of exocytic events occur from docked DCVs. (A) Number of vesicles in a subset of stimulated cells (13 cells, 177 events) that we classified as docked or newcomer. 60% of the vesicles are docked. We used particle tracking software (Mosaic, ImageJ) to track vesicles prior to stimulation. Vesicles were classified as docked if they were tracked for a full fifteen, continuous frames before exocytosis and otherwise classified as newcomers. This method almost certainly underestimates the number of docked vesicles; if a vesicle fell below the detection threshold used for only a single frame it was not counted as docked. (B) The average mean square displacement is plotted against time for all tracks from docked vesicles. This is fit with a straight line with a slope of 36*10-4 μm2/s, which gives a diffusion coefficient of 9*10-4 μm2/s, which is consistent with previous measurements of DCV diffusion parameters in neuroendocrine cells and indicates the vesicles are strongly docked at the plasma membrane (Lang et al. 2000. Biophysical Journal 78: 2863-2877).

SI Figure 6

Rab27a

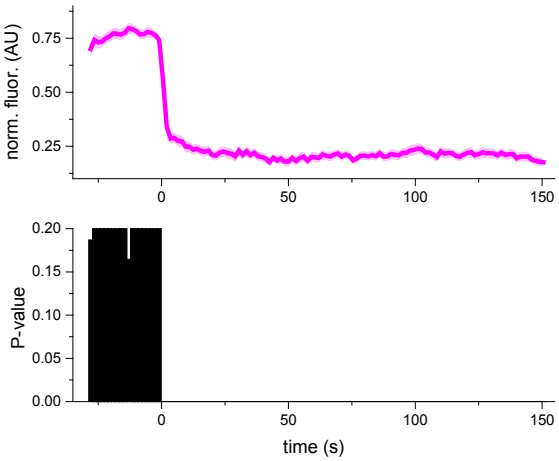

time (s)

-8.5 -1 6.5

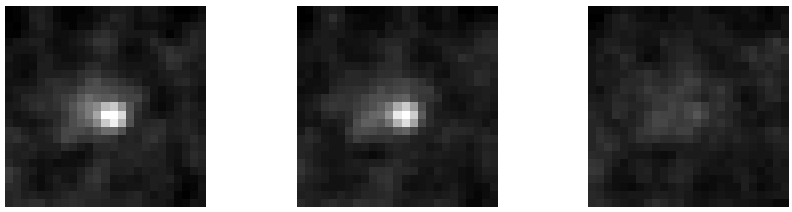

Rab3a

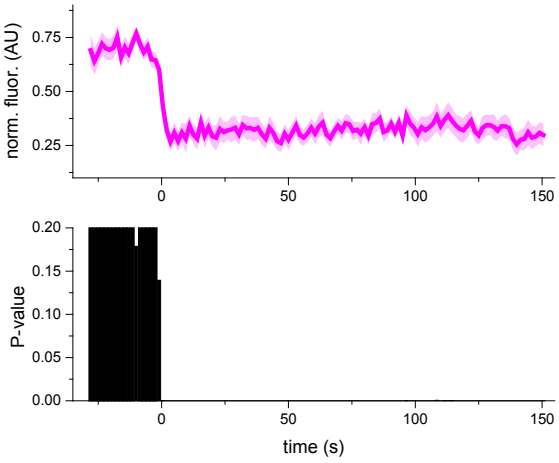

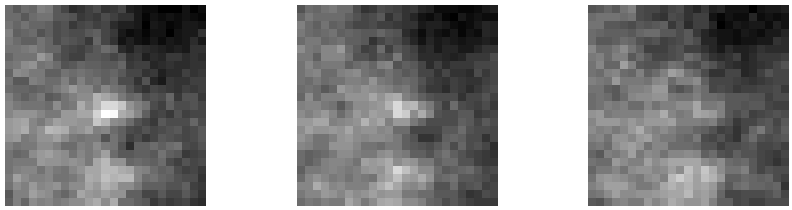

Rabphilin3a

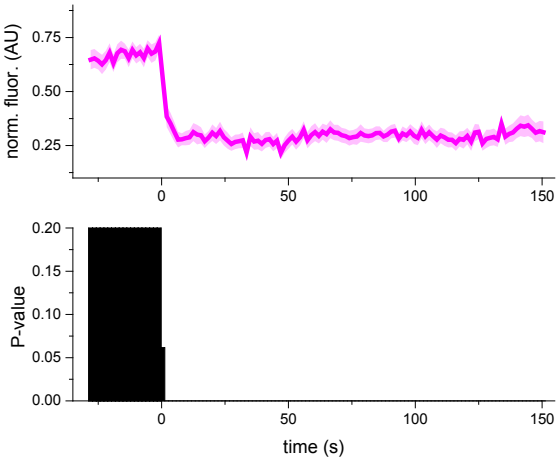

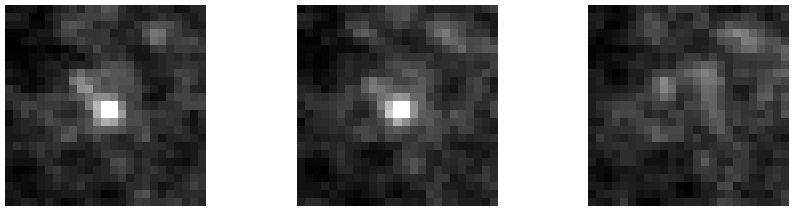

mCherry

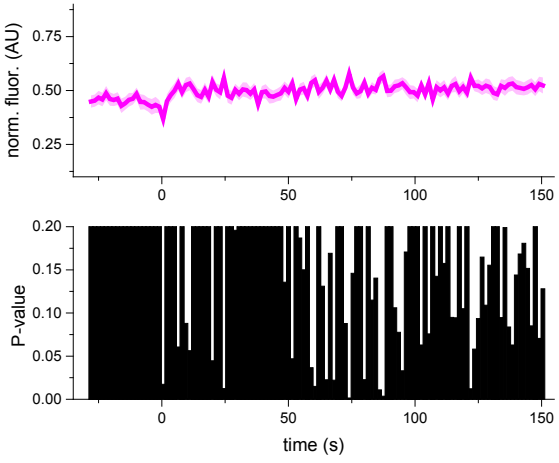

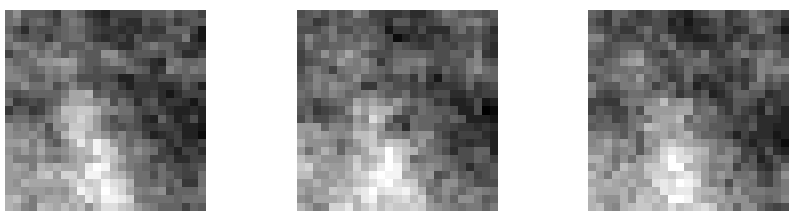

SI Figure 6

munc18a

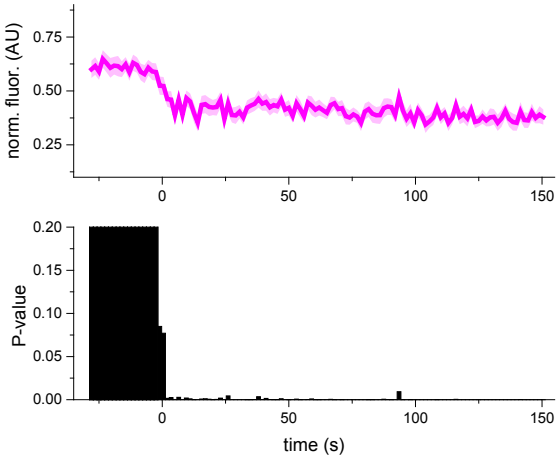

time (s)

-8.5 -1 6.5

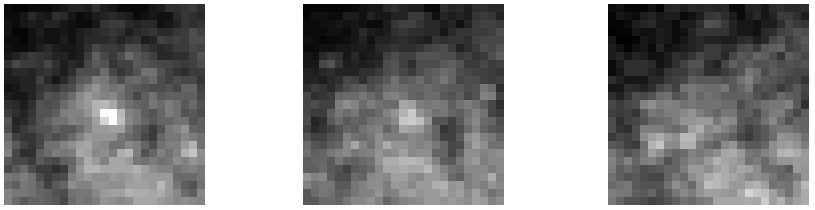

tomosyn

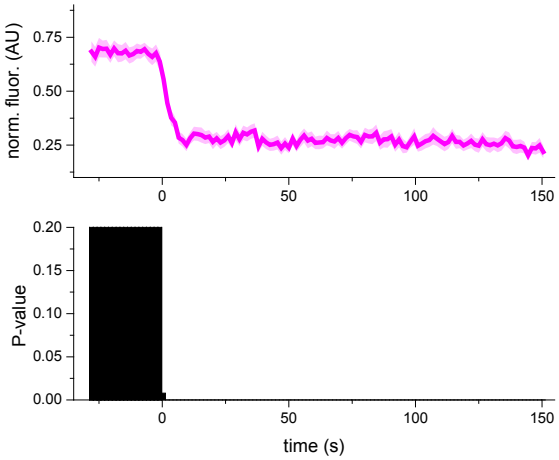

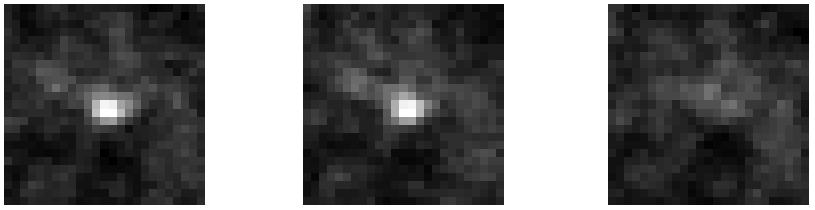

CAPS

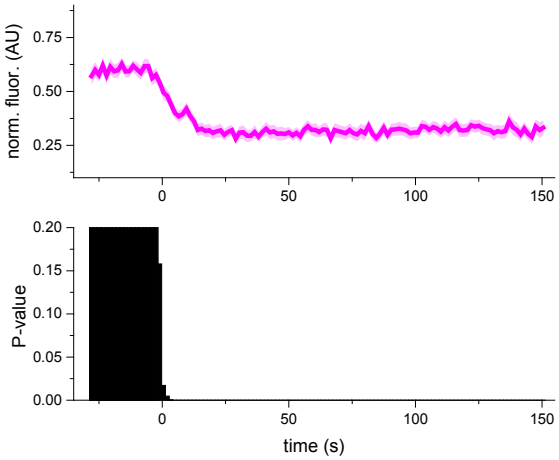

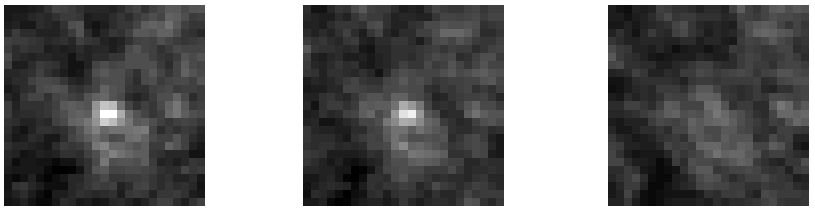

SI Figure 6

Dnm1

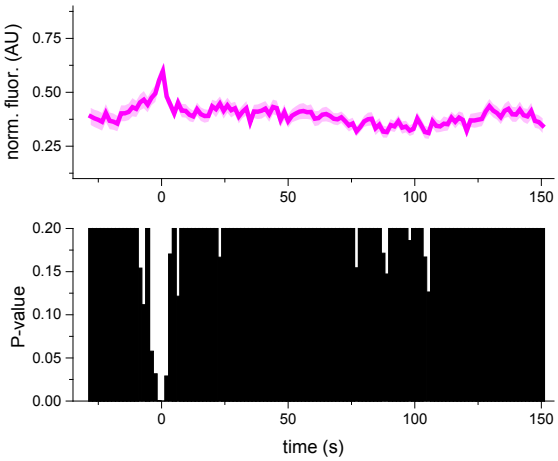

time (s)

-8.5 -1 6.5

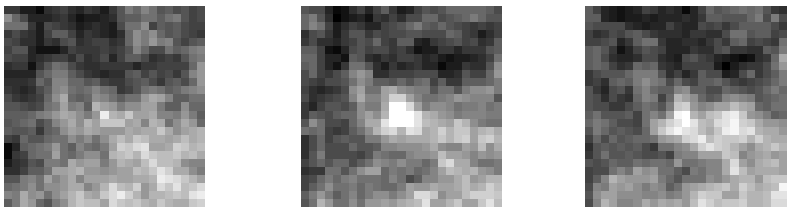

Dnm2

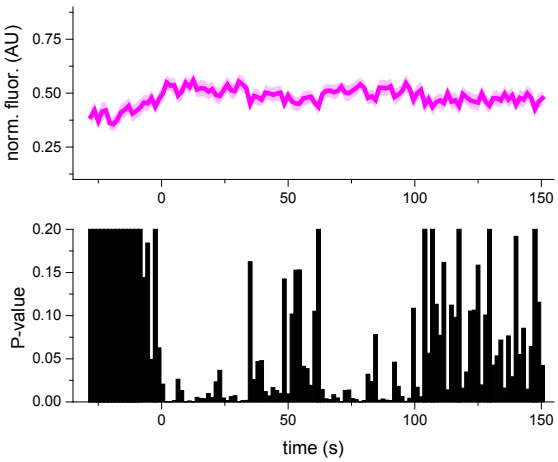

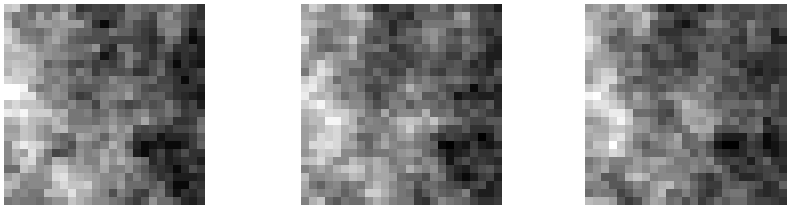

PIP2-sensor

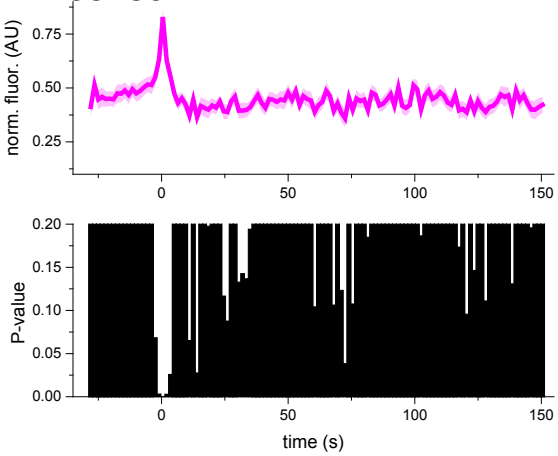

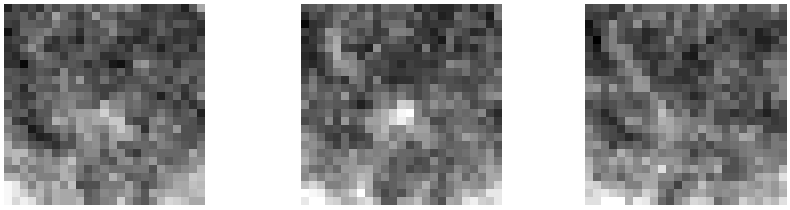

Amphiphysin

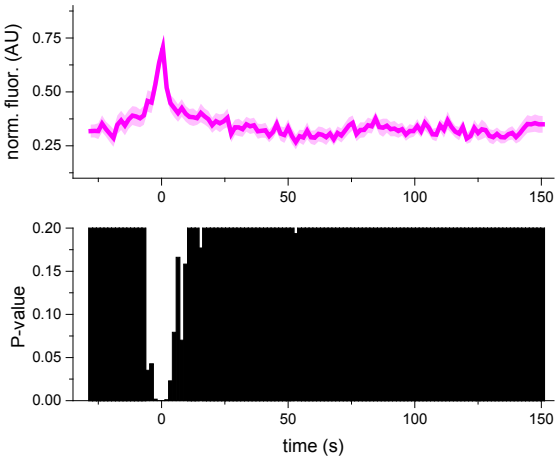

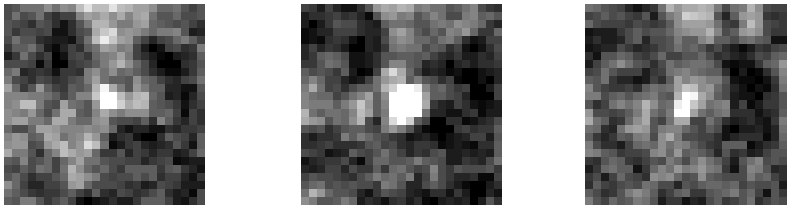

SI Figure 6

Syndapin

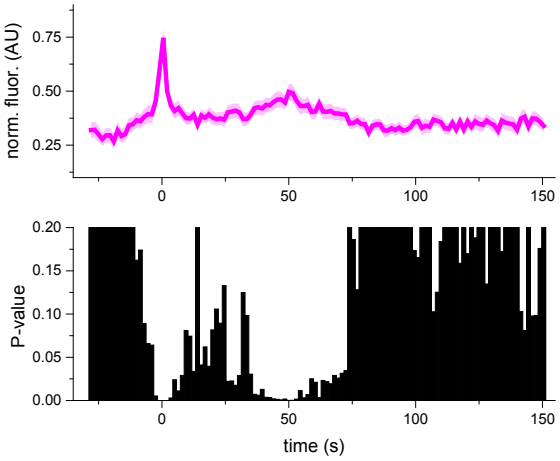

time (s)

-8.5 -1 6.5

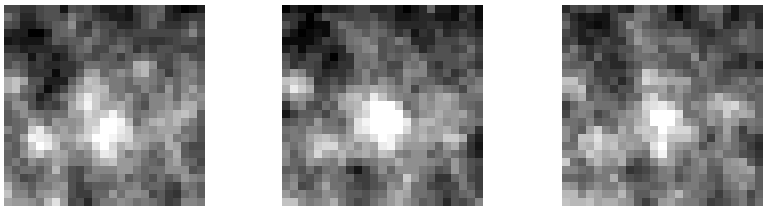

Endophilin A2

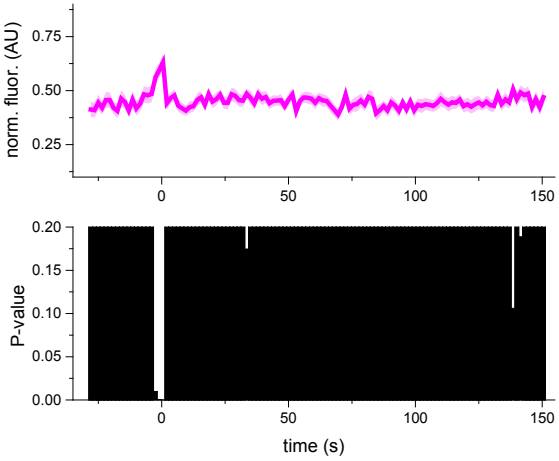

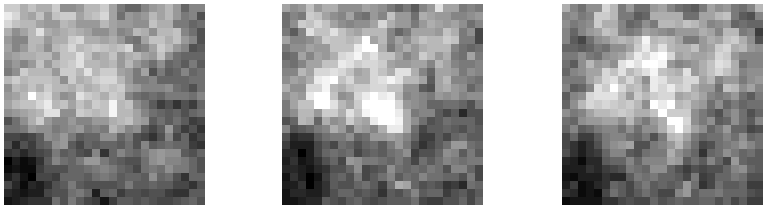

farn-mCherry

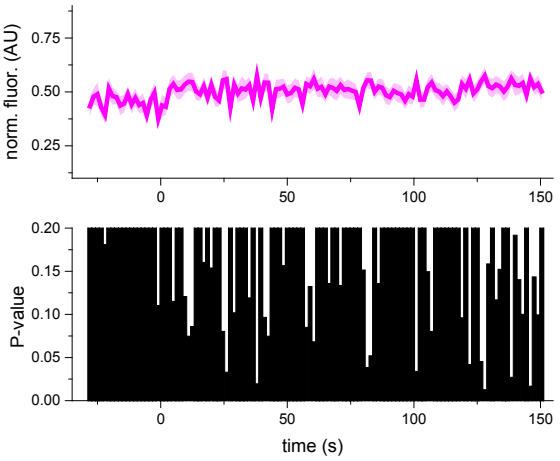

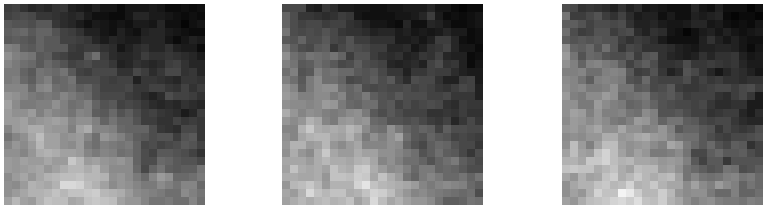

SI Figure 6

Dnm1-K535A

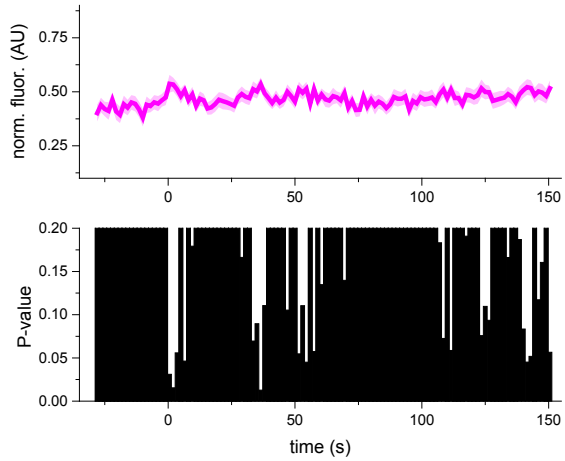

time (s)

-8.5 -1 6.5

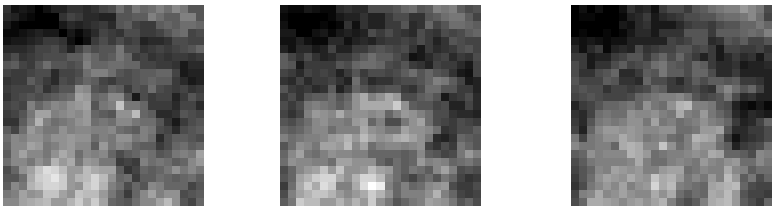

Dnm1-S774E-S778E

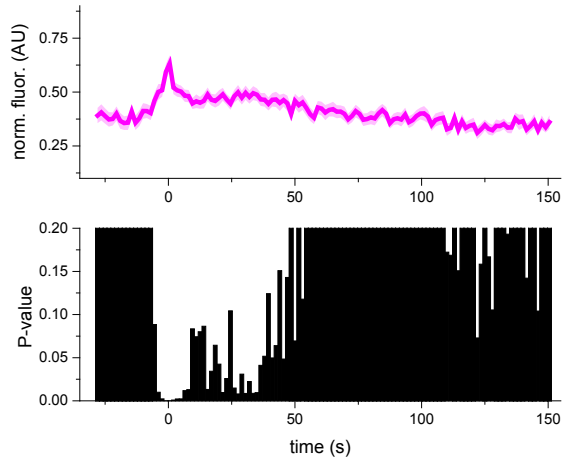

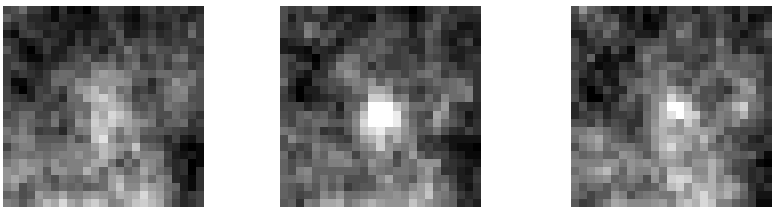

Dnm1-833-838A

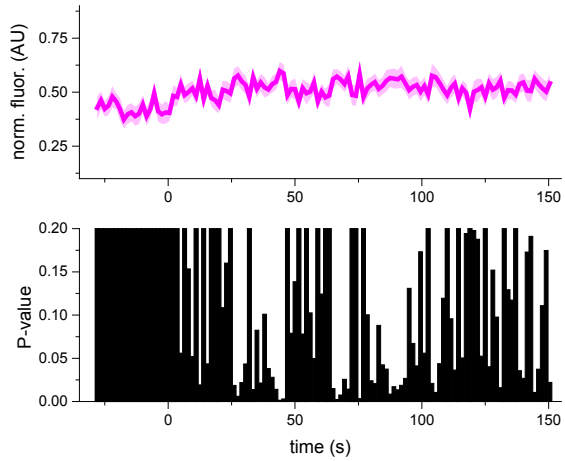

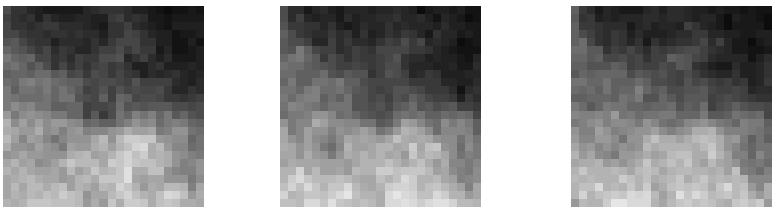

Dnm1-K44A

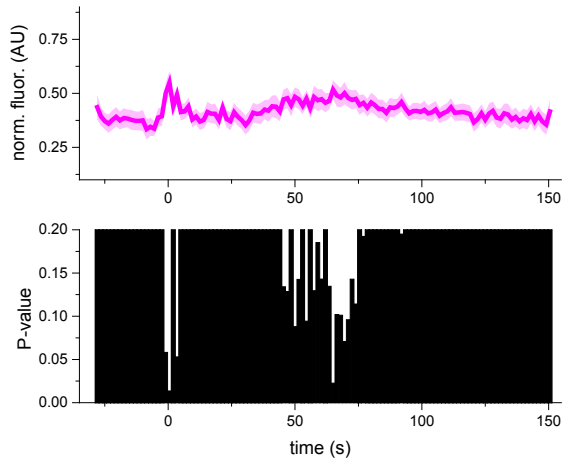

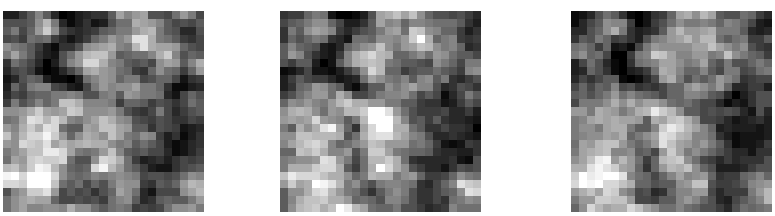

SI Figure 6

Dnm2-K535A

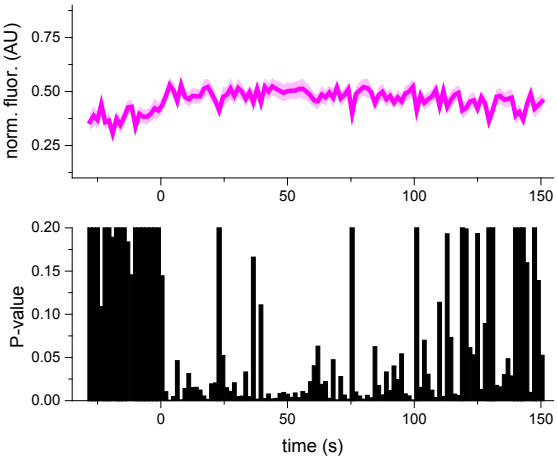

Dnm2-dPRD

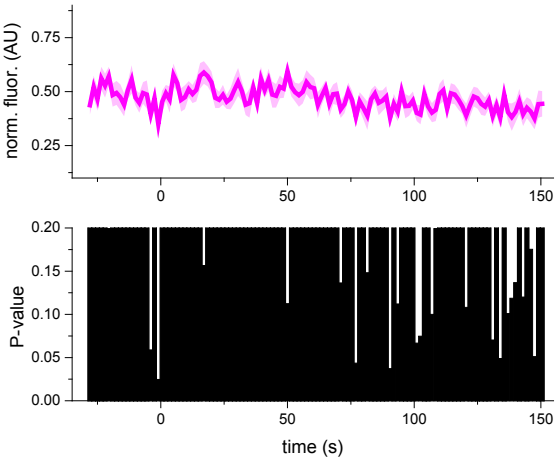

time (s)

-8.5 -1 6.5

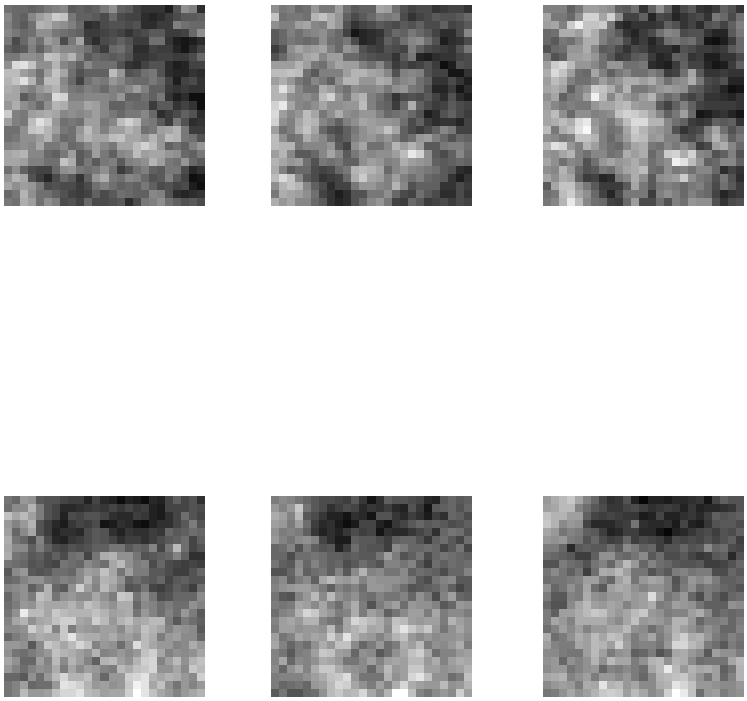

SI Figure 6

syntaxin1a

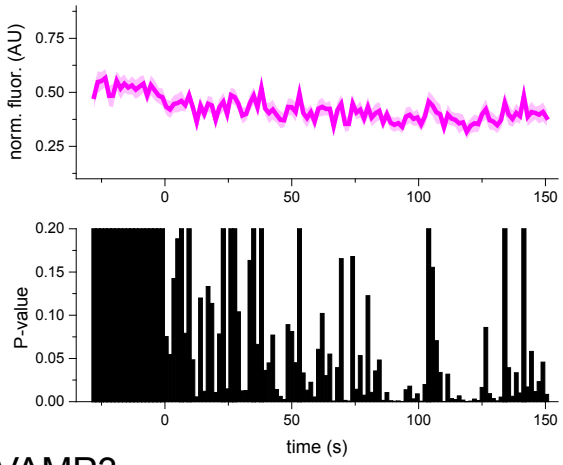

complexin

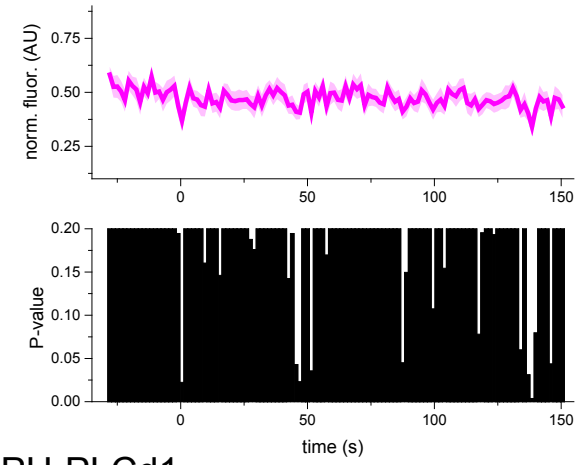

VAMP3

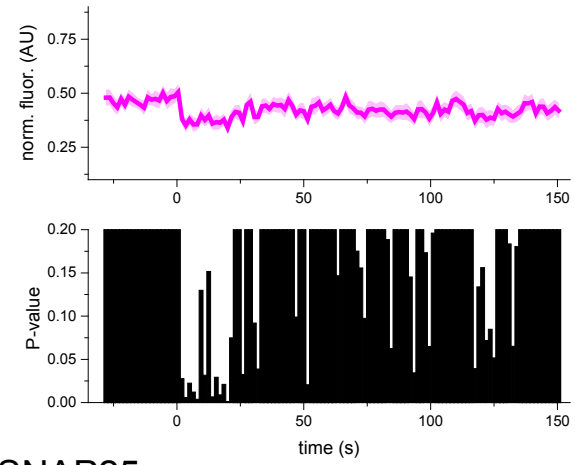

PH-PLCd1

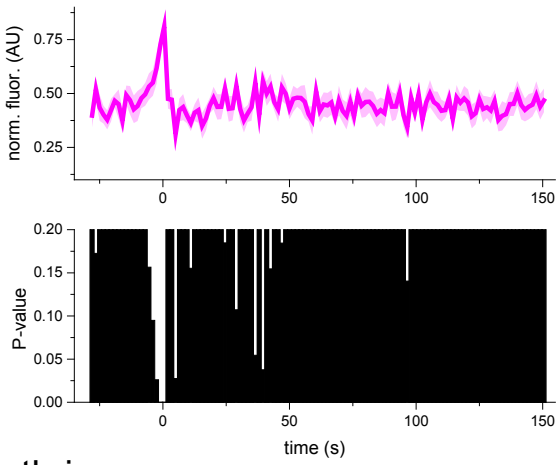

SNAP25

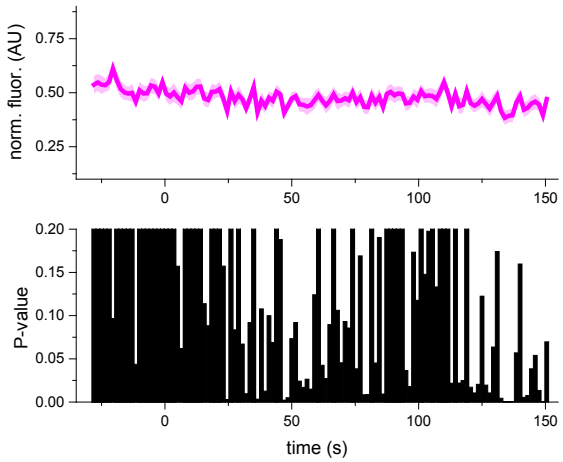

clathrin

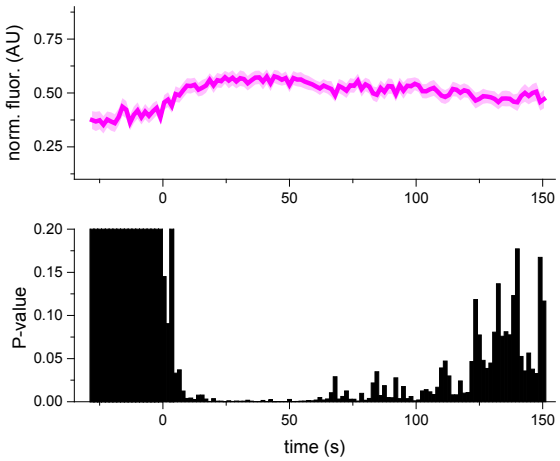

synaptotagmin-1

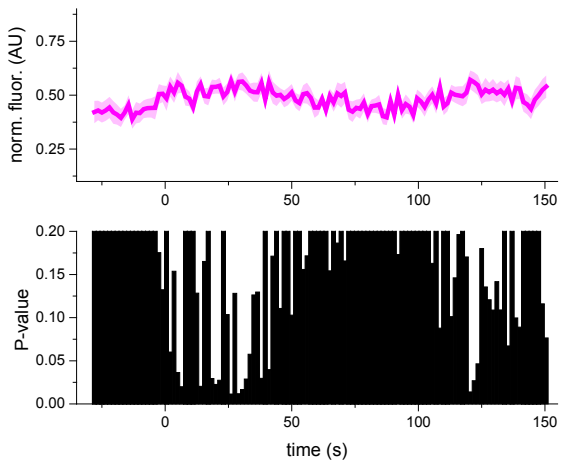

phogrin

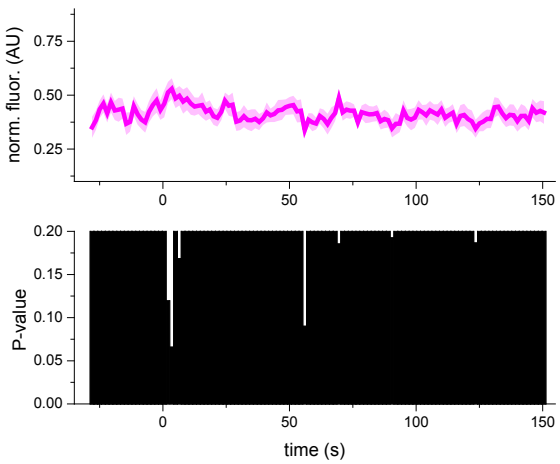

SI Figure 6

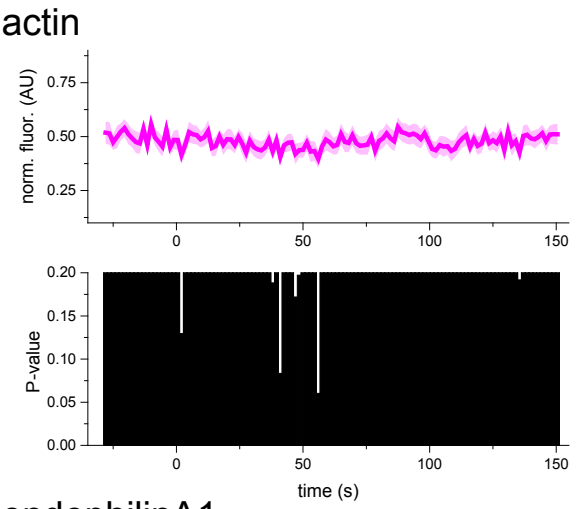

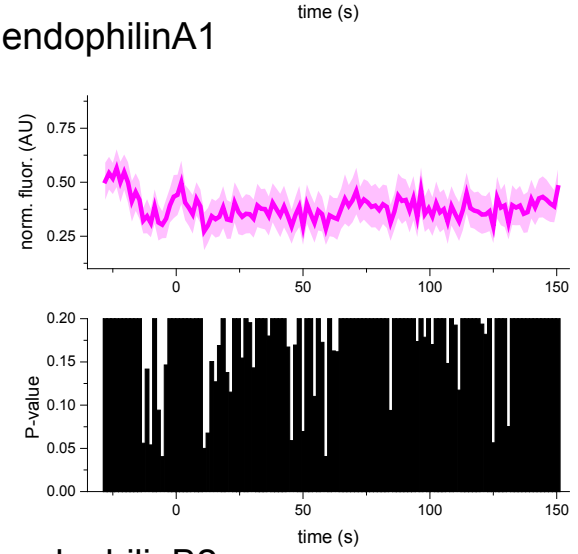

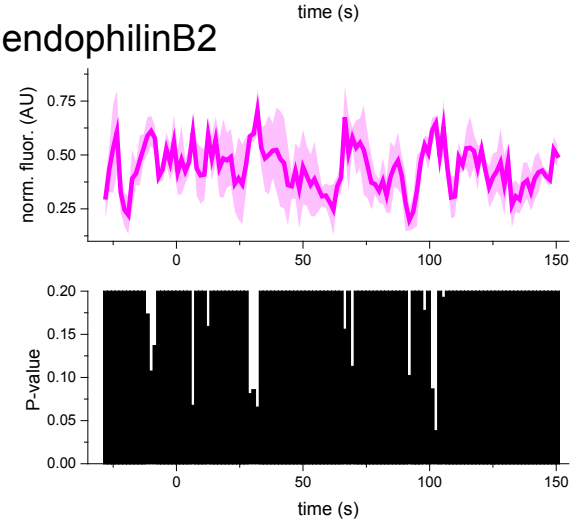

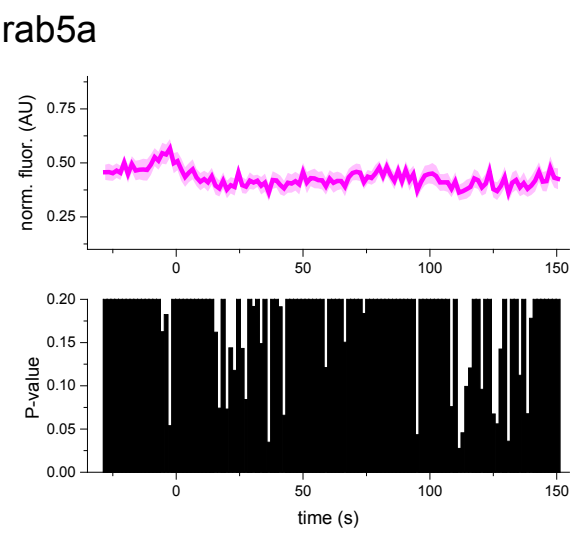

SI Figure 6: Full-length fluorescence intensity trajectories of all proteins of interest in exocytosis. Top left of each panel is the background subtracted and normalized fluorescence intensity traces for protein indicated, note the Y-axis scale is smaller than in the main text. Many of these are shown at shorter timescales in the main text to highlight the timescale where dynamic intensity changes occur (centered around the time of fusion). The mean fluorescence intensity is shown as a dark line and the standard error of the dataset is shown in transparency behind the data. If the standard error is not visible it is smaller than the line. Bottom left of each panel is a plot of T-test P-value versus time for the trajectory. A baseline average intensity was calculated for each trajectory by averaging the first ten data points in each individual trajectory that makes up the average intensity trajectory. Then, across the dataset the intensity at each timepoint was compared against the baseline intensity value using a Student's T-Test. The P-value is plotted against time. We interpret P-values of less than 0.05 to suggest that the intensity at the timepoint is statistically distinguishable from the average intensity at the beginning of the trajectory. At right of each panel for proteins from the main text are average image frames for before, near, and after the time of membrane fusion (t=0). Interestingly, mCherry is mildly recruited after exocytosis, which is consistent with previous observations (Taraska et al. 2003. PNAS 100: 2070-2075). Presumably a docked DCV and the assembled exocytic machinery physically occlude mCherry (and other cytoplasmic molecules) and after exocytosis, some of the space can be occupied by cytoplasmic mCherry. Importantly, clathrin light chain appears to be recruited to a greater extent than mCherry, which suggests that clathrin is specifically associating with the exocytic site instead of merely assembling at space recently vacated by the DCV.

SI Figure 7

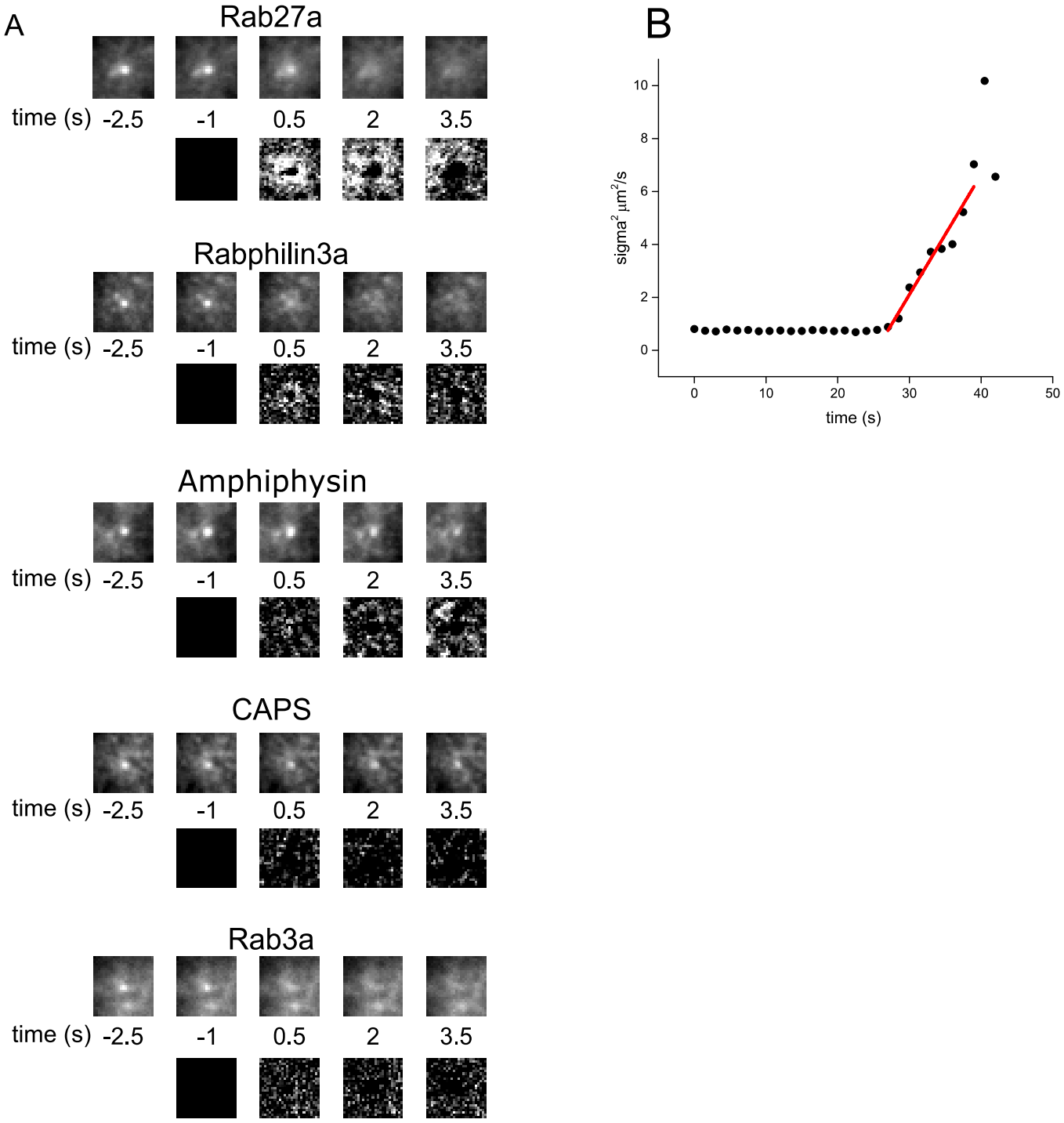

SI Figure 7: Rab27a, but not other proteins, diffuses away from the exocytic site in the plane of the membrane. (A) Top of each panel, consecutive frames of an average movie of exocytosis from the indicated construct are shown (n values for the average are listed in Figure SI 1B). No background subtraction or normalization was applied to movie shown before averaging, though similar results were obtained with normalization. Time values are the same as shown in fluorescence intensity trajectories in Figures 3-5. Bottom of each panel, average movie frames with the frame prior to fusion subtracted. This was done to better visualize spreading of fluorescence in a lateral wave from the exocytic site (as in Rab27a). Many of the proteins analyzed show little to no evidence of the lateral wave evident in the Rab27a panel. (B) Plot of width of a Gaussian fit to the Rab27a signal against time. The diffusion of particles from a point source within a plane is well described. When this is imaged the particle distribution is convolved with the PSF of the microscope, which can be fit with a Gaussian distribution. The width parameter of the Gaussian profile can be fit to obtain an estimate of the diffusion coefficient of the particles. A Gaussian fit to the Rab27a profile (radially averaged line scan) is stable until exocytosis after which the protein begins diffusing outwards, increasing the width of the Gaussian fit. Points on the plot of Gaussian width parameter over time corresponding to the frames after fusion are fit with a straight line, the slope of which gives the diffusion coefficient (Zenisek et al. 2002. Neuron 35: 1085-1097). Similar treatment of the other proteins shown resulted in plots that could not be fit with a straight line, further suggesting that these proteins do not diffuse away from the exocytic site in the plane of the membrane.

SI Figure 8

A

	offset (y0)	A1	t1	Reduced Chi-Sqr	Adj. R-Square
WT	0.25106	0.5574	44.2026	7.22E-04	0.96519
Dnm1-K535A	0.1392	0.69836	23.629	7.51E-04	0.97094
Dnm1-833-838A	0.21041	0.65869	28.6448	2.85E-04	0.98857
Dnm1-K44a	0.19653	0.6283	37.8006	9.00E-04	0.96499
Dnm1-S774E-S778E	0.20447	0.60556	32.7986	2.56E-04	0.9886
Dnm2-K535A	0.25576	0.60036	40.0313	2.87E-04	0.98762
Dnm2-dPRD	0.15717	0.74426	30.9498	2.39E-04	0.99272
Dnm2-siRNA treat	0.21105	0.66108	21.1652	2.40E-04	0.99087

B

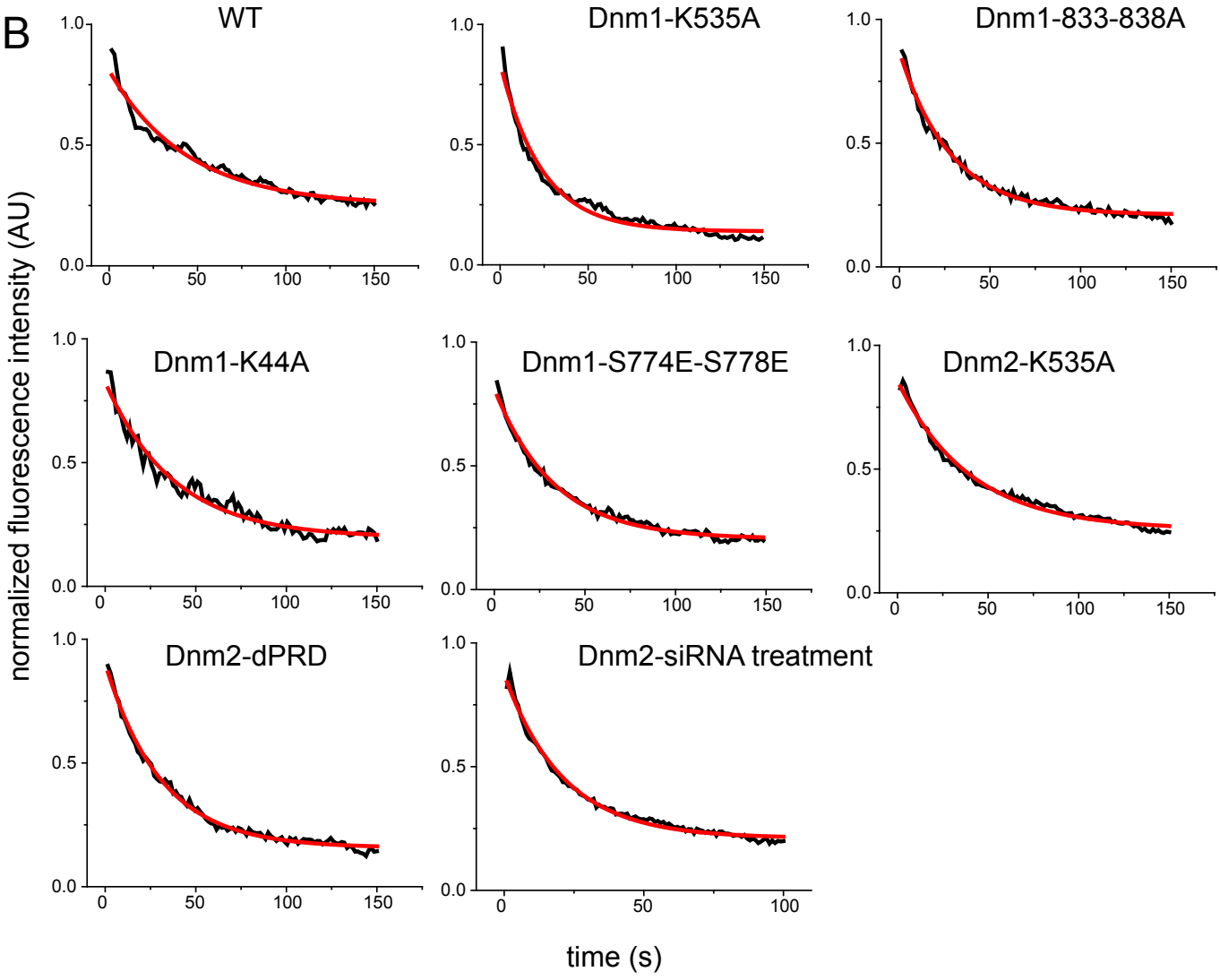

SI Figure 8: Fitting of tPA-GFP decays post-fusion in INS-1 cells. A) Table of fitting parameters and statistical measures of goodness-of-fit, fitting was performed in Origin software using the equation: y=A*exp(-x/t1) + y0. B) tPA-GFP decays (black lines), beginning at t=1.5 seconds, are fit with single component exponential decays (red lines).